

Sub-wavelength GaN-based membrane high contrast grating reflectors

Tzeng Tsong Wu,¹ Yu Cheng Syu,² Shu Hsien Wu,¹ Wei Ting Chen,³ Tien Chang Lu,^{1,*}
Shing Chung Wang,¹ Hai Pang Chiang,^{4,5} and Din Ping Tsai,^{3,6,7}

¹Department of Photonics & Institute of Electro-Optical Engineering, National Chiao Tung University, Hsinchu 30050, Taiwan

²Institute of Display, National Chiao Tung University, Hsinchu 30050, Taiwan

³Graduate Institute of Applied Physics, National Taiwan University, Taipei 10605 Taiwan

⁴Institute of Optoelectronic Sciences, National Taiwan Ocean University, Keelung 20245, Taiwan

⁵Institute of Physics, Academia Sinica, Taipei 115, Taiwan

⁶Department of Physics, National Taiwan University, Taipei 10617, Taiwan

⁷Research Center for Applied Sciences, Academia Sinica, Taipei 115, Taiwan

timtulu@mail.nctu.edu.tw

Abstract: The GaN-based membrane high contrast grating (HCG) reflectors have been fabricated and investigated. The structural parameters including grating periods, grating height, filling factors and air-gap height were calculated to realize high reflectivity spectra with broad bandwidth by the rigorous coupled-wave analysis and finite-difference time-domain method. Based on the optimized simulation results, the GaN-based membrane HCGs were fabricated by e-beam lithography and focused-ion beam process. The fabricated GaN-based membrane HCG reflectors revealed high reflectivity at 460 nm band with large stopband width of 60 nm in the TE polarization measured by using the micro-reflectivity spectrometer. The experimental results also showed a good agreement with simulated ones. We believe this study will be helpful for development of the GaN-based novel light emitting devices in the blue or UV region.

©2012 Optical Society of America

OCIS codes: (050.0050) Diffraction and gratings; (050.6624) Sub-wavelength structures; (220.4241) Nanostructure fabrication.

References and links

1. T. C. Lu, C. C. Kao, H. C. Kuo, G. S. Huang, and S. C. Wang, "CW lasing of current injection blue GaN-based vertical cavity surface emitting laser," *Appl. Phys. Lett.* **92**(14), 141102 (2008).
2. T. C. Lu, S. W. Chen, T. T. Wu, P. M. Tu, C. K. Chen, C. H. Chen, Z. Y. Li, H. C. Kuo, and S. C. Wang, "Continuous wave operation of current injected GaN vertical cavity surface emitting lasers at room temperature," *Appl. Phys. Lett.* **97**(7), 071114 (2010).
3. D. Kasahara, D. Morita, T. Kosugi, K. Nakagawa, J. Kawamata, Y. Higuchi, H. Matsumura, and T. Mukai, "Demonstration of blue and green GaN-based vertical-cavity surface-emitting lasers by current injection at Room Temperature," *Appl. Phys. Express* **4**(7), 072103 (2011).
4. A. J. Shaw, A. L. Bradley, J. F. Donegan, and J. G. Lunney, "GaN resonant cavity light-emitting diodes for plastic optical fiber applications," *IEEE Photon. Technol. Lett.* **16**(9), 2006–2008 (2004).
5. G. S. Huang, T. C. Lu, H. H. Yao, H. C. Kuo, S. C. Wang, C. W. Lin, and L. Chang, "Crack-free GaN/AlN distributed Bragg reflectors incorporated with GaN/AlN superlattices grown by metalorganic chemical vapor deposition," *Appl. Phys. Lett.* **88**(6), 061904 (2006).
6. C. Mateus, M. Huang, L. Chen, C. Chang-Hasnain, and Y. Suzuki, "Broad-band mirror (1.12–1.62 μm) using a subwavelength grating," *IEEE Photon. Technol. Lett.* **16**(7), 1676–1678 (2004).
7. M. C. Y. Huang, Y. Zhou, and C. J. Chang-Hasnain, "A surface-emitting laser incorporating a high-index-contrast subwavelength grating," *Nat. Photonics* **1**(2), 119–122 (2007).
8. R. G. Mote, S. F. Yu, W. Zhou, and X. F. Li, "Design and analysis of two-dimensional high-index-contrast grating surface-emitting lasers," *Opt. Express* **17**(1), 260–265 (2009).
9. Y. Zhou, M. C. Y. Huang, C. Chase, V. Karagodsky, M. Moewe, B. Pesala, F. G. Sedgwick, and C. J. Chang-Hasnain, "High-index-contrast grating (HCG) and its applications in optoelectronic devices," *IEEE J. Sel. Top. Quantum Electron.* **15**(5), 1485–1499 (2009).

10. M. C. Y. Huang, Y. Zhou, and C. J. Chang-Hasnain, "Nano electro-mechanical optoelectronic tunable VCSEL," *Opt. Express* **15**(3), 1222–1227 (2007).
11. M. C. Y. Huang, Y. Zhou, and C. J. Chang-Hasnain, "A nanoelectromechanical tunable laser," *Nat. Photonics* **2**(3), 180–184 (2008).
12. V. Karagodsky, B. Pesala, C. Chase, W. Hofmann, F. Koyama, and C. J. Chang-Hasnain, "Monolithically integrated multi-wavelength VCSEL arrays using high-contrast gratings," *Opt. Express* **18**(2), 694–699 (2010).
13. C. Chase, Y. Rao, W. Hofmann, and C. J. Chang-Hasnain, "1550 nm high contrast grating VCSEL," *Opt. Express* **18**(15), 15461–15466 (2010).
14. J. H. Lee, S. M. Ahn, H. J. Chang, J. H. Kim, Y. S. Park, and H. S. Jeon, "Polarization-dependent GaN surface grating reflector for short wavelength applications," *Opt. Express* **17**(25), 22535–22542 (2009).
15. J. H. Kim, D. U. Kim, J. H. Lee, H. S. Jeon, Y. S. Park, and Y. S. Choi, "AlGaIn membrane grating reflector," *Appl. Phys. Lett.* **95**(2), 021102 (2009).
16. M. G. Moharam and T. K. Gaylord, "Rigorous coupled-wave analysis of planar-grating diffraction," *J. Opt. Soc. Am.* **71**(7), 811–818 (1981).
17. K. S. Yee, "Numerical solution of isitial boundary value problems involving Maxwell's equations in isotropic media," *IEEE Trans. Antennas Propag.* **AP 14**(3), 302–307 (1966).
18. W. C. Lin, L. S. Liao, H. Chen, H. C. Chang, D. P. Tsai, and H. P. Chiang, "Size dependence of nanoparticle-SERS enhancement from silver film over nanosphere (AgFON) Substrate," *Plasmonics* **6**(2), 201–206 (2011).
19. W. T. Chen, C. J. Chen, P. C. Wu, S. Sun, L. Zhou, G. Y. Guo, C. T. Hsiao, K. Y. Yang, N. I. Zheludev, and D. P. Tsai, "Optical magnetic response in three-dimensional metamaterial of upright plasmonic meta-molecules," *Opt. Express* **19**(13), 12837–12842 (2011).
20. W. T. Chen, P. C. Wu, C. J. Chen, H. Y. Chung, Y. F. Chau, C. H. Kuan, and D. P. Tsai, "Electromagnetic energy vortex associated with sub-wavelength plasmonic Taiji marks," *Opt. Express* **18**(19), 19665–19671 (2010).
21. T. M. Babinec, J. T. Choy, K. J. M. Smith, M. Khan, and M. Lončar, "Design and focused ion beam fabrication of single crystal diamond nanobeam cavities," *J. Vac. Sci. Technol. B* **29**(1), 010601 (2011).
22. M. Bass and the Optical Society of America, *Handbook of Optics*, 3rd ed. (McGraw-Hill, 2009).

1. Introduction

Over the past decade, GaN-based optoelectronic devices such as resonant cavity light-emitting diodes (RCLEDs) and vertical cavity surface emitting lasers (VCSELs) have been investigated and developed for many different applications [1–4]. One of the important ingredients of RCLEDs and VCSELs is the high reflectivity reflector for forming high quality factor cavity structures. Distributed Bragg reflectors (DBRs) consisted of multiple-pair index-contrast materials is one of the choices for cavity reflectors. However, III-N based DBRs were challenged to fabricate due to the lattice-mismatch problem and small index difference between GaN and AlN material systems. The epitaxial growth of crack-free high reflectivity GaN/AlN DBRs have been demonstrated by insertion of the superlattice for strain relaxation in 2006 [5]. The complex epitaxial structure and narrow stopband width in the reflectivity spectra were still issues to be solved. On the other hand, the high contrast grating (HCG) reflectors have been recently developed and investigated because of their superior properties such as highly reflectivity with large bandwidth, polarization control and light mass for fast tuning of cavity modes [6–9]. Up to now, HCG have been demonstrated in several III-V systems and applied on different optoelectronic devices. In recent years, HCG structures have been integrated to 850 nm VCSELs and tunable HCG VCSELs [7, 10, 11]. Besides, HCG VCSELs have further been explored to operate at 1550 nm for optical communications and wavelength division multiplexing applications [12, 13].

As for the HCG development in the short-wavelength region, the GaN surface grating reflectors have been proposed for the wavelength range in the blue band. But the reflectivity of the surface grating reflectors only reached to 90% [14]. Besides, the AlGaIn membrane grating reflectors have been realized by photoelectrochemical (PEC) etching of the underlying InGaIn sacrificial layer for the wavelength range in the green band [15]. However, the PEC etching strongly depended on material properties of the InGaIn sacrificial layer and it would bring up several challenges such as difficulty in fabrication of thick InGaIn epitaxial structures to form a thick underlying air-gap. So the thickness of air-gap would be limited to 200 nm, resulting in low reflectivity (~80%) due to the insufficient air-gap height. Here, we reported the GaN-based membrane HCG reflectors with a thick undercut air-gap using e-

beam lithography (EBL) and focused-ion beam (FIB) process. The rigorous coupled-wave analysis (RCWA) [16] and finite-difference time-domain (FDTD) method [17, 18] were used to calculate the optimized parameters for fabrication of the high reflectivity GaN-based membrane HCG. In fabrication, the GaN-based membrane HCG reflectors with a thick air-gap were fabricated by EBL [19, 20] and FIB process [21]. The large thickness of air-gap could inhibit severe reduction on the stopband bandwidth of reflectivity spectrum. Finally, the reflectivity spectra in TE and TM polarization were measured by the micro-reflectivity spectrometer. The experimental results showed a similar tendency with the simulation ones.

2. Design and Simulation

The schematic of the GaN-based membrane HCG is shown in Fig. 1. We assumed that both transverse electric (TE; electric field direction parallel to the grating lines) and transverse magnetic (TM; electric field direction perpendicular to the grating lines) polarized lights would incident from the air side to the HCG structure in the normal direction. The optimized structure was designed to maximize the reflectivity (TE polarization) at $\lambda = 460$ nm. The main parameters including grating period (Λ), grating height (H), filling factor (FF, grating width divided by the period) and air-gap height (AH) were considered in the calculation. The refractive index dispersion of GaN was applied by using the Sellmeier equation [22].

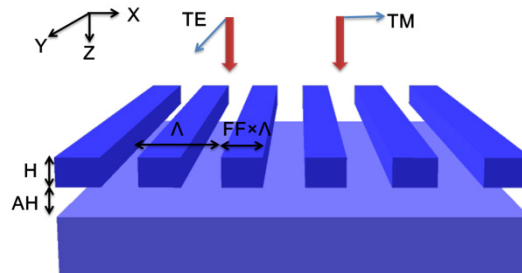


Fig. 1. The schematic of the GaN-based membrane high contrast grating. The blue arrows show the E-field polarization direction.

We first performed the RCWA calculations on the GaN-based membrane HCG shown in Fig. 1 to find the optimum structural parameters. The detailed optimization process was similar to the previous reports [6, 14]. The optimized structure parameters have been determined as follows: the grating period (Λ) was 405 nm; the grating height (H) was 160 nm; the filling factor (FF) was 0.525; and the air-gap height (AH) was 400 nm. Figures 2(a) and 2(b) plot the diffraction efficiency spectra of the optimized structure for the TE and TM polarized lights, respectively. The reflectivity reached to 99% at 460 nm for the TE polarization. On the contrary, the reflectivity for TM-polarized light showed the spectrum obviously different from the TE-polarized results. This suggested that the optimized GaN-based membrane HCG reflector could achieve high reflectivity with good polarization selectivity. The reason of high reflectivity could be described as follows: when the wavelength of incident wave equals to or large than the grating period, energy of the high order diffractions would be suppressed. So it would only exhibit the reflected or transmitted wave in the normal direction to the surface. Hence, as the wave propagates through the sub-wavelength grating with proper design, it will experience the destructive interference while the phase difference is π between the index contrast materials. So it will lead the reflectivity approaching to almost 100% with little transmittance [9, 14]. To further analyze the reflectivity spectrum in Fig. 2(a), the spectral stopband width $\Delta\lambda_R$ for the reflectivity larger than 99% could reach 45 nm. It indicates that the GaN-based membrane HCG reflector is superior to the surface type grating reflector for which the stopband width was only 20 nm [14] due to the insufficient total reflection conditions at the top side of the HCG. Therefore,

the GaN-based membrane HCG could be excellent for serving as the high reflectivity reflectors of GaN-based VCSEL or other novel photonic devices.

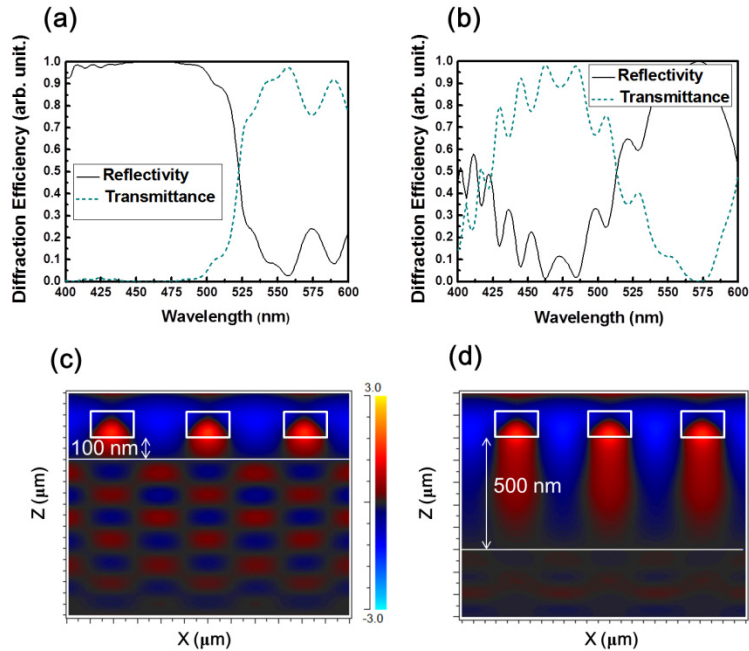


Fig. 2. The simulated diffraction efficiency spectra of the GaN-based membrane high contrast grating (optimized for $\lambda = 460$ nm) (a) TE-polarization and (b) TM-polarization. The electric field distribution in y-axis around the high contrast grating region for incident wavelength of 460 nm with TE-polarization light when (c) air-gap is 100 nm and (d) air-gap is 500 nm.

Next, the FDTD method was employed to investigate the electric field (E_y) distribution of GaN-based membrane HCG with incident wavelength at 460 nm. The electric field distributions of GaN-based membrane HCG reflectors with air-gaps of 100 and 500 nm are shown in Fig. 2(c) and Fig. 2(d), respectively. It should be noted that the incident lights came from the top air side in the FDTD calculations. Figure 2(c) shows the incident wave would transmit through the HCG structure because the air-gap thickness is insufficient for supporting the destructive interference. On the contrary, it can be observed that almost no electromagnetic energy could transmit through the HCG with the air-gap of 500 nm in Fig. 2(d). It suggests that the destructive interference is perfect for the membrane HCG reflector with a large air-gap.

To consider the difficulty in actual nano fabrication process, the fabrication tolerance of different structural parameters in the GaN-based membrane HCG reflectors were calculated. The influences of various parameters on the reflectivity spectra including the grating period (Λ), grating height (H), filling factor (FF), and air-gap height (AH) of GaN-based membrane HCG reflectors were discussed as shown in Fig. 3. Figure 3(a) indicates that the grating period should approach the designed wavelength to reach high reflectivity spectra. For the grating height mapping shown in Fig. 3(b), it is worth mentioning that grating height has high tolerance for fabrication process around 460 nm. The large stopband spectra with reflectivity greater than 90% can be observed over the grating height ranging from 120 nm to 180 nm. On the other hand, as shown in Fig. 3(c), the high reflectivity could be only observed when the filling factor ranges from 0.5 to 0.525, making the filling factor to be the most sensitive parameter in the HCG fabrication. We can learn from Fig. 3(d) that high reflectivity over 99% with a 76 nm wide stopband width can be obtained when the air-gap height is greater than

400 nm. On the contrary, the value of reflectivity gradually decreases when the air-gap height is less than 200 nm.

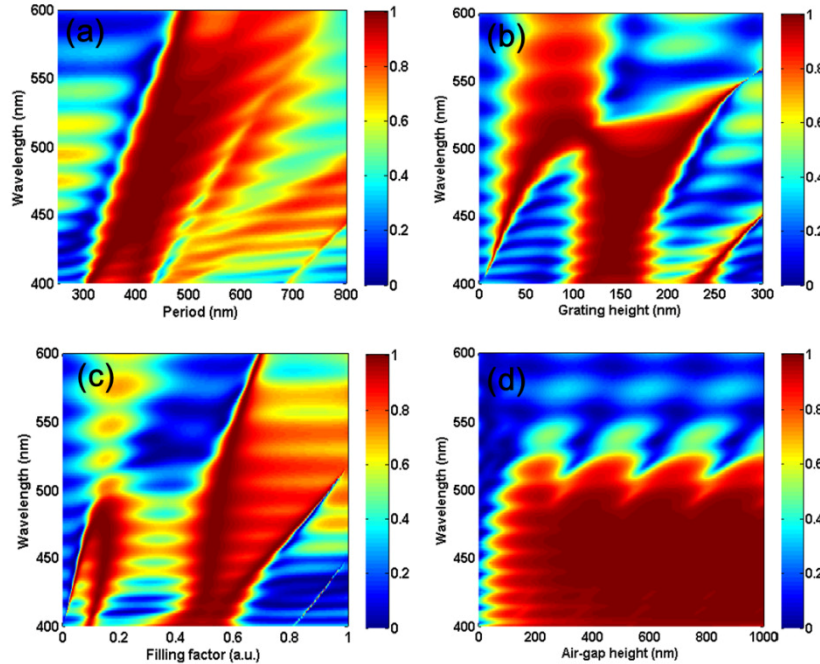


Fig. 3. Reflectivity spectra mappings of the GaN-based membrane HCG reflectors (optimized for $\lambda = 460$ nm TE-polarization) for various structural parameters: (a) grating period, (b) grating height, (c) filling factor, (d) air-gap height.

3. Results and Discussion

The epitaxial structure for fabrication of the GaN-based membrane HCG reflector was grown by a low pressure metal-organic chemical-vapor-deposition system. A 2.5 μm thick un-doped GaN layer was grown on a c-plane sapphire substrate. As for the fabrication process, firstly, a 200 nm SiN_x layer was deposited as a hard mask on the top of the as-grown sample by plasma-enhanced chemical vapor deposition. Then, a 300 nm PMMA layer as the soft mask was coated on the sample by spin coating. After that, the grating patterns were defined on the PMMA by EBL. Then the SiN_x layer was etched down to reveal the GaN surface using reactive-ion etching (RIE). The induced-coupled plasma (ICP) was used to etch the GaN layer for about 200 nm deep. The area of the patterned HCG was designed to be 400 μm^2 . The SiN_x layer was removed by the buffered oxide etch (BOE) dipping. Finally, we employed the FIB to fabricate the membrane structure with large air-gap height by tilting the sample for ion-beam etching. Figures 4(a), 4(b) and 4(c) show the scanning electron microscope (SEM) images of the final results for the plane view and the tilted angle view. The parameters estimated by the SEM images are as followed: $\Lambda \sim 410$ nm, $H \sim 160$ nm, $FF \sim 0.524$, and $AH \sim 800$ nm, which are closed to the designed values.

To further analyze the reflectivity spectra of the GaN-based membrane HCG reflector, the micro-reflectivity spectrometer was used to measure the reflectivity in the TE/TM polarization. The micro-reflectivity spectrometer contained one light source (Halogen lamp; 12 V, 100 W), one polarizer, one analyzer, and one 100X objective lens as a condenser. Moreover, the silver mirror was used as a reference for calibration of the reflectivity spectra. In measurement, the white light emitted from the Halogen lamp passed through the polarizer and then was split into two beams via a 50/50 beam splitter (BS). The reflected beam would

be directed into the 100X objective lens with a numerical aperture (N.A.) of 0.9 and then was focused on the sample and silver mirror, respectively. The spot size was estimated to be $400 \mu\text{m}^2$ which was fitted to the area of the membrane HCG. Then, light reflected from the sample (or silver mirror) was collected by the objective lens and passed through the analyzer. Finally the collected light would be fed into a photometer tube to record the reflectivity spectrum. The reflectivity spectra with TE or TM polarization could be distinguished by the polarizer and analyzer.

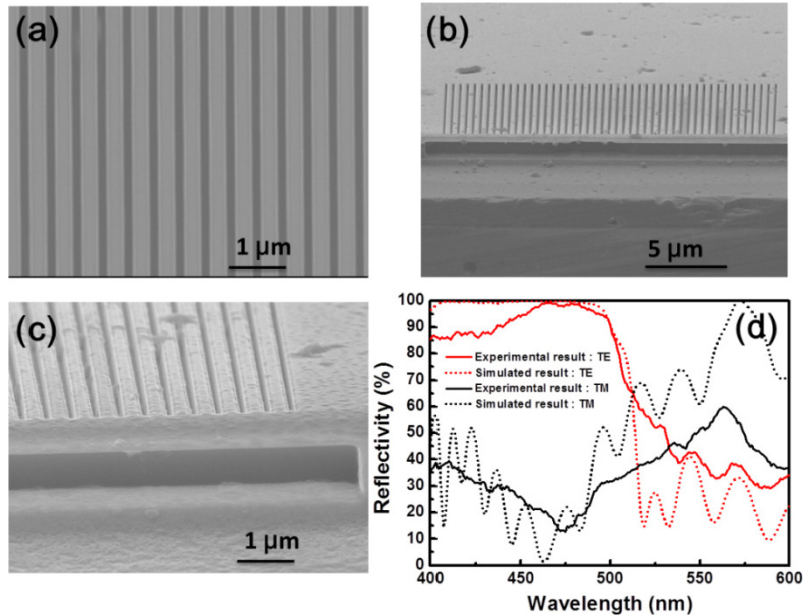


Fig. 4. SEM images for (a) top view, (b) tilted angle view and (c) enlarged tilted angle view of the GaN-based membrane HCG reflector. (d) Experimental and simulated reflectivity spectra of the GaN-based membrane HCG reflector for both TE and TM polarizations.

Figure 4(d) shows the measured and simulation reflectivity spectra of the GaN-based membrane HCG reflector for TE/TM polarizations. The red solid line shows the measured reflectivity spectrum in TE polarization. The difference between the simulation and experimental results could be attributed to the tapered sidewalls of GaN-based membrane HCG reflectors. During the etching process, the sidewalls of grating would form trapezoid shapes and the filling factor thus changed accordingly, which would modify the reflectivity spectrum of membrane HCG. Nevertheless, the reflectivity with the TE polarization was greater than 0.9 with a stopband width of $\Delta\lambda_R \approx 60 \text{ nm}$ (from 440 nm to 500 nm). On the contrary, the black solid line shows the measured reflectivity spectrum in TM polarization which exhibits only 10% reflectivity at 460 nm. The extinction ratio of TE/TM polarization is greater than 9, suggesting that the GaN-based membrane HCG reflector has good polarization selectivity. The presented results were consistent with the simulations and should be helpful for realization of the blue-violet HCG VCSELs and other novel photonic devices.

4. Conclusion

In summary, the GaN-based membrane HCG reflectors have been designed and fabricated. The optimized parameters have been calculated and analyzed to reach high reflectivity with TE polarization using RCWA and FDTD methods. The large fabrication tolerance is helpful for reduction the difficulties in the process. Moreover, the GaN-based membrane HCG reflectors with large air-gaps have been fabricated by the EBL and FIB process. The

reflectivity spectra with TE/TM polarization were measured by micro-reflectivity spectrometer. The measured reflectivity spectrum for TE polarization showed a large stopband width of about 60 nm with reflectivity over 90%. The measured results were in good agreement with the simulation results. We believe the presented results provide great potential for applications on the GaN-based photonic devices and could be helpful for realization of GaN-based HCG VCSELs and other novel photonic devices in the near future.

Acknowledgments

This work was supported in part by the Ministry of Education Aim for the Top University program and by the National Science Council of Taiwan under Contract No. NSC99- 2622-E009-009-CC3 and NSC98-2923-E-009-001-MY3. The authors would like to acknowledgment Prof H. C. Kuo from National Chiao Tung University for his technical support and Prof F. Koyama from Tokyo Institute of Technology for his kind suggestion.